

Surface Roughness Optimization of Selective Laser Melting printed 17-4 PH Stainless Steel Parts

Priya Sahadevan¹, Chithirai Pon Selvan², Amiya Bhaumik¹ and Avinash Lakshmikanthan^{3*}

¹Lincoln University College, Selangor - 47301, Malaysia

²School of Science and Engineering, Curtin University, Dubai - 345031, United Arab Emirates

³Department of Mechanical Engineering, Nitte Meenakshi Institute of Technology, Bengaluru - 560064, Karnataka, India; avinash.l@nmit.ac.in

Abstract

The 17-4 PH stainless steel possesses distinguished applications due to its inherent properties. Higher surface roughness in Selective Laser Melting (SLM) parts limits their use in a wide range of applications. Higher surface roughness deteriorates the important functional properties (strength, fatigue, corrosion resistance and so on). Therefore, an attempt is being made to reduce the surface roughness during the processing stage itself, rather than the dependency of costly secondary post-processing routes. Taguchi L9 experiments are conducted to analyze the laser power, scan speed and hatch distance influence on the surface roughness of SLM parts. Laser power showed the highest percentage contribution equal to 83.37%, followed by scan speed of 9.92% and hatch distance of 6.71%, respectively. Taguchi method determined optimal conditions (laser power: 270 W, scan speed: 1000 mm/s and hatch distance: 0.08 mm) through Pareto analysis of variance resulted in low values of surface roughness with a value equal to 4.11 μm . The results of the optimal condition can be used by any novice user to obtain better surface quality in SLM parts. Further, the Taguchi method can be applied to optimize any process with limited experimental trials and resources.

Keywords: Pareto ANOVA, SLM Process, Surface Roughness, Taguchi Method, 17-4 PH Stainless Steel

1.0 Introduction

The Additive Manufacturing (AM) process employs a computer to design the three-dimensional object to create models (i.e., replicas of the actual part) and build complex products (which are often difficult to process with traditional manufacturing routes) with machines at reduced cost and time^{1,2}. AM technology is classified majorly into three processing routes such as liquid (fused deposition modelling, stereolithography), solid (laminated object manufacturing) and powder (binder jetting, selective laser route (melting and sintering, electron beam melting and so on)^{2,3}. The Selective Laser Melting (SLM) technique combines the desirable features

of both casting (rapid heating and cooling with short duration at liquid state) and powder metallurgy (ensures homogeneous mixing and milling of metal powders resulting in particle fracture and deformation causes cold welding and powder compaction) techniques to build the metal parts^{4,5}. The effective use of powdered material with the possibility to recycle and reuse unmelted powders are the other potential advantages of the SLM technique⁶. Surface remelting occurs during the SLM process, which affects the surface chemistry of the part resulting in a thick surface oxide layer (external skin) leading to higher surface roughness^{7,8}. SLM technology build parts are widely accepted in many industrial parts (such as aerospace, automotive, marine, jewellery and so

*Author for correspondence

on)⁹. Precipitate-hardened steels (in particular, 17-4 PH stainless steel) possess distinguished properties and are therefore being widely used in structural and commercial engineering applications¹⁰⁻¹³. However, the surface quality of 17-4 PH steels-based SLM build parts is found inferior which limits most of the engineering applications and requires significant research attention¹⁴.

In recent years a significant amount of research efforts has been made to improve the surface quality of printed parts *viz.* theoretical, traditional experimental and statistical design of experiment approaches. The theoretical mathematical model was developed to predict the surface roughness of steel 316L alloy, with a set of parameters (layer thickness, sharpness)¹⁵. The developed model did not predict the optimal parameters for minimum surface roughness. Central composite design-based experiments are performed to study the influencing parameters (laser power: LP, scan speed: SS, and scan spacing) on the surface roughness of build parts¹⁶. Full factorial design-based experimental trials are performed by conducting a set of factors (LP, SS, and scan spacing) on the surface roughness of aluminium alloy build parts¹⁷. The effect of process parameters (LP, SS, layer thickness: LT, slope angle: SA) on the surface roughness of Hastelloy X parts¹⁸. SLM parameters (LP, SS, energy density) were examined on the surface roughness of AlSi 10Mg parts¹⁹. The traditional or try-error experimental approach increases the trial runs with an increased set of variables that maximizes the cost because of generated wastes (material, labour, energy, time and so on)²⁰⁻²³. Furthermore, the detailed analysis (significance or non-significance) of process variables and their optimal variables on the surface roughness is not fully solved in the literature. In addition, common efforts made to reduce the surface roughness by analyzing parameters resulted in different optimal conditions for different materials¹⁶⁻¹⁹. This occurs because of the difference in material melting temperature and properties, and therefore the levels of variables are found to be different.

The study of the surface roughness of different materials is of industrial relevance due to their detrimental effect on the corrosion and fatigue properties of aluminium alloy²⁴. Lower surface roughness of Ti6Al4V alloy-based SLM parts resulted in increased dimensional accuracy and density²⁵. Surface roughness reduced from 39 to 0.13 μm , and showed increased strength (tensile, yield) and

ductility in the printed parts²⁶. The secondary processing techniques (sandblasting and chemical etching) applied to improve the surface quality of the biomedical part (Ti6Al4V alloy) resulted in enhanced strength and ductility in the built parts²⁷. However, secondary, or post-processing could increase the overall cost of the built products. Therefore, minimizing the surface roughness without the requirement of post-processing techniques is of industrial relevance.

From the above literature review, the following observations are noticed: higher surface roughness in build parts affects fatigue, dimensional accuracy, tensile strength, and corrosion resistance properties. Therefore, higher surface roughness limits the use of the parts in many engineering applications. Although secondary post-processing techniques reduce the surface roughness with simultaneous improvement in strengths and other properties, provide compromising at a higher cost. Therefore, the present work aims to study the process variables (LP, SS, and hatch distance: HD) at reduced experimental trials utilizing the Taguchi method. The significance of each variable is analyzed on the surface roughness of 17-4 PH stainless steel build parts. Furthermore, optimal parametric conditions are determined that could reduce the surface roughness with limited practical experiments at reduced wastes (labour hours, material, and energy waste). The practical suitability of the model is tested and validated by conducting experiments. The optimal conditions that result in low surface roughness are recommended to industries.

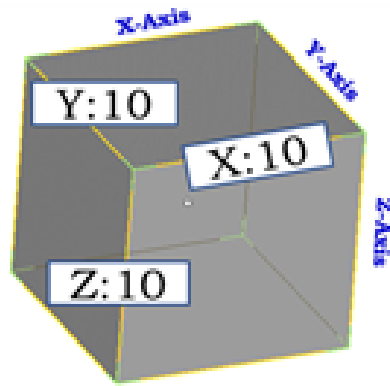
2.0 Materials and Methodology

The 17-4 PH stainless steel finds major applications in aerospace, biomedical applications, dental implants, impellers, hydraulic piston pumps, chemical, and food processing industrial applications²⁸⁻³¹. The chemical composition possessing the main alloying elements is presented in Table 1.

Selective Laser Melting (SLM) is an advanced manufacturing process used for creating complex and precise metal parts. In the current work, SLM samples are built by fusing thin layers of metal powder of 17-4PH SS using a high-power laser, layer by layer, based on a digital model. This technique enables the

Table 1. Chemical elements of 17-4PH Steel

Elements	Wt. (%)
Cr	15-17.5
Ni and Cu	3-5 each
Mn and Si	Max. 1.0 each
Nb	0.15 – 0.45
Mo	Max. 0.5

**Figure 1.** Schematic representation of cube dimension of printed parts.

production of parts with complex geometries and fine details, unachievable through traditional manufacturing methods.

The 17-4 PH Stainless Steel metal powders were used to print the SLM parts. The metal powders are procured from the local supplier possessing $\sim 50 \pm 10 \mu\text{m}$ powder size. SLM 280 machines were used to fabricate the samples possessing a cube dimension of $10 * 10 * 10$ mm. A schematic representation of the cube specimen is presented in Figure 1. During experimentation, the laser spot diameter, operation beam focus, minimum scan line and layer thickness were maintained constant equal to 0.2 mm, 100 μm , 100 μm , and 40 μm , respectively. The control factors that influence the surface roughness of build parts are varied according to the Taguchi experimental matrix and recorded surface roughness data to conduct analysis and optimization. The most influencing parameters and operating levels on surface roughness are determined by performing trial-run experiments and referring to published literature¹⁶⁻¹⁹. The parameters and levels defined

Table 2. Control variables and levels

Variables	Levels (low:1, medium:2 and high:3)
Laser power	240, 270, 300 W
Scan speed	600, 800, 1000 mm/s
Hatch distance	0.08, 0.10, 0.12 mm

for developing the model performing the analysis and optimizing the process are presented in Table 2. Similar parameters were chosen by Sheshadri *et al*¹⁴.

3.0 Experimental Details and Measurements

Experiments are performed for the set of three process variables and their operating levels utilizing the Taguchi L_9 matrix. Three replicate experiments are conducted for each set of conditions.

Table 3. Surface roughness of 17-4PH stainless steel parts

Exp. No.	LP, W	SS, mm/s	HD, mm	Surface Roughness, μm
L ₁	240	600	0.08	9.37 ± 0.31
L ₂	240	800	0.10	8.43 ± 0.24
L ₃	240	1000	0.12	7.73 ± 0.18
L ₄	270	600	0.10	6.35 ± 0.17
L ₅	270	800	0.12	5.42 ± 0.18
L ₆	270	1000	0.08	4.11 ± 0.13
L ₇	300	600	0.12	5.34 ± 0.15
L ₈	300	800	0.08	4.97 ± 0.12
L ₉	300	1000	0.10	5.67 ± 0.10

Surface roughness measurements are performed on the SLM build parts possessing cube dimensions (1 cm^3) using a surface roughness tester. Mitutoyo surfest SJ-210 testing equipment was used to record the surface roughness data on as-built 17-4 PH stainless steel specimens. The sampling length to record the surface roughness data is 2.5 mm on the build sample. A total of

24 surface roughness data (8 roughness data on each cube x 3 replicate experiment) is recorded at each experimental condition and the average surface roughness (Ra) value is used to perform analysis and optimization (Table 3). In addition, optical profilometry (Veeco NT910, USA) is used to know the three-dimensional surface profile of printed parts. The instrument accuracy of optical profilometry is 0.1 nm in Z resolution and 1% as step height accuracy.

4.0 Result and Analysis

Taguchi L_9 experimental matrices were used to record the input-output data. The results of experimental data were analyzed to examine the parametric significance. Pareto analysis of variance was used to perform factor analysis and determine optimal parametric conditions responsible for lower surface roughness on the printed samples.

4.1 Data Collection and Analysis

Experiments are conducted according to the L_9 matrices of the Taguchi method. Taguchi L_9 matrices are selected for experimentation, as there are mainly the three most influencing variables (LP, SS, HD) operating at respective three levels. The surface roughness values are recorded to correspond to each experimental condition (Table 3). The measured surface roughness data is transformed to Signal-to-Noise (S/N) ratio data by selecting lower-the-better quality characteristics utilizing Equation (1). Note that lower surface roughness on the printed parts is desirable to ensure better properties (strength, fatigue, corrosion resistance and so on). The computation of the S/N ratio (represented with η_{ij}) corresponding to i^{th} experimental condition of j^{th} output is done using Equation (1).

$$S / N_{SR} = \eta_{ij} = -10 \log \left(\frac{1}{n} \sum_{i=1}^n (y_{ij})^2 \right) \quad (1)$$

$$n = 1, 2, \dots, m; j = 1, 2, \dots, p$$

In Equation (1), the terms p and m represent the number of responses and experimental runs. The measured surface roughness data transformed to S/N ratio data utilizing Equation (1) for all L_9 experiments is presented in Table 4.

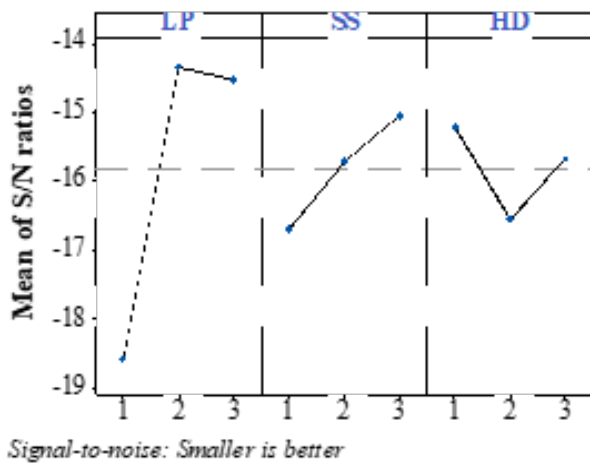
Table 4. Surface roughness of 17-4PH stainless steel parts

Exp. No.	Surface Roughness (μm)	S/N Ratio (dB)
L_1	9.37 ± 0.31	-19.43
L_2	8.43 ± 0.24	-18.52
L_3	7.73 ± 0.18	-17.76
L_4	6.35 ± 0.17	-16.06
L_5	5.42 ± 0.18	-14.68
L_6	4.11 ± 0.13	-12.28
L_7	5.34 ± 0.15	-14.55
L_8	4.97 ± 0.12	-13.93
L_9	5.67 ± 0.10	-15.07

The analysis of the significance of factors on the response (output) is of industrial relevance to know the complete detailed process insights. The S/N ratio data corresponding to actual surface roughness data is used to analyze the factor significance. Pareto analysis of variance table is constructed comprising of the Sum of Factor Levels (SFL), the Sum of Squares of Differences (SSD), Per cent Contribution (PC) and optimal condition for each factor. Higher values of the S/N ratio are desirable for better quality characteristics (i.e., lower surface roughness in the printed part). In other words, low values of surface roughness are always the result of a higher S/N ratio. To know the factor significance the sum of each level of an individual factor is estimated. The SSD corresponds to each factor that could help to determine the PC of that factor. A higher PC value indicates the most significant parameter (i.e., change in the factor levels shows maximum changes in surface roughness in the printed parts) towards surface roughness. If the PC of the individual factor is less than 5%, then that parameter is insignificant when tested at a preset confidence level of 95% (P-value < 0.05). Optimal conditions for the SLM process are determined based on the SFL values of each factor. Higher values of SFL indicate the optimal levels correspond to that factor. The summary of the results of the Pareto analysis of variance for surface roughness is presented in Table 5. Based on the Table 4 S/N ratio data, Table 5 was constructed. The percentage contribution for a factor is computed based on SSD. (i.e.,

Table 5. Pareto ANOVA results for surface roughness

Factors	Levels	LP	SS	HD	Total
SFL	1	-55.7	-50.1	-45.6	-142.3
	2	-43.0	-47.1	-49.6	
	3	-43.6	-45.1	-47.0	
SSD		309.6	36.9	24.9	379.4
PC		83.37	9.92	6.7	100
OL		LP ₂ SS ₃ HD ₁			

**Figure 2.** Main factor effects based on mean values of S/N ratio data.

Percent Contribution (PC) for LP = SSD of LP/SSD of total).

The effect of individual factors is determined based on the computing values of levels of each factor (Figure 2). All factors had a significant effect on surface roughness, as their percentage contribution was found to be greater than 5%. Laser power showed the highest contribution with 83.37%, followed by scan speed and hatch distance equal to 9.92%, and 6.7%, respectively.

The effect of individual factors on surface roughness, when varied between their respective levels is presented in Figure 2. Low and high values of laser power resulted in lesser surface roughness values. Low laser power results in lesser energy and may not be sufficient to melt all metal powders which results in voids or porous, microporosity, coarse shape of solidified tracks and discontinuities

which causes higher surface roughness on the build parts¹⁷. In addition, lesser energy density values as a result of lower laser power generate a small quantity of liquid with high viscosity and remains a liquid state for a very short duration causing large size irregular pores i.e., rough surface on build parts^{32,33}. Higher values of laser power (i.e., 300 W) resulted in higher energy density which tends to remelt the already solidified molten pool, burn of material, and vaporization of materials causing spherical pores or discontinuities or adhered material on the build parts³⁴. The said reasons create the rough surface on the build parts. The surface roughness values decreased with the increased values in scan speed from 600 to 1000 mm/s. A higher scan speed at 1000 mm/s may not have sufficient time to remelt the already solidified melt pool, and all metal powders that melt with large quantities possessing the lowest viscosity ensure to fill of the small pores resulting in a better surface finish in the build part. Similar observations are reported in the published literature³⁵. An increase in hatch distance resulted in an increase in surface roughness on the SLM build parts (Figure 2). This occurs because the overlap between the melt track decreases with increased values of hatch distance resulting in rough surface on build parts³⁶. The levels of factors responsible for reduced surface roughness determine the optimal condition for surface roughness. The laser power, scan speed and hatch distance maintained equal to 270 W, 1000 mm/s and 0.08 mm, are the optimal conditions to yield better surface roughness in the SLM process. The optimal condition derived from the Pareto analysis of variance was found to be one of the parametric conditions of L₉ experiments (i.e., Exp. No.: L₆). Therefore, the Taguchi method is efficient in

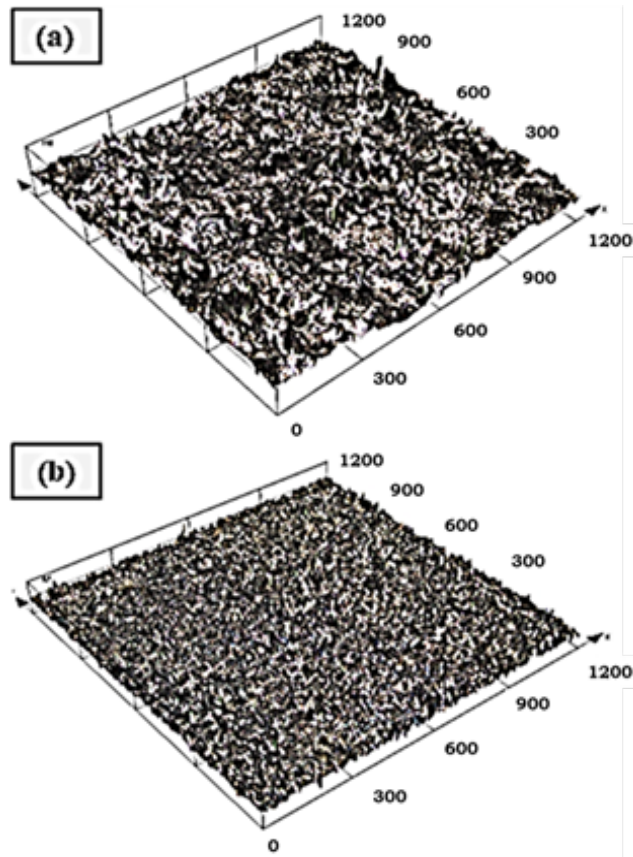


Figure 3. Surface roughness of 17-4PH Steel parts: (a) initial condition (Table 3, Exp. No.: L_1) and (b) Optimal condition (Table 3, Exp. No.: L_6) determined by Taguchi method.

optimizing the process with limited experimental trials for obtaining better surface quality in the build parts. The optimal condition resulted in a smooth surface compared to the initial experimental conditions (Figure 3).

5.0 Conclusion

PH stainless steels possess major applications in medical and many engineered parts. The surface roughness of building parts directly affects the mechanical and other functional properties. Therefore, attempts are being made to reduce the surface roughness to conduct minimum experiments without the need for costly secondary processing routes (polishing, coating, sandblasting and so on). The following conclusions are drawn from the obtained results:

- The effects of SLM factors (laser power, scan speed and hatch distance) were analyzed by conducting only 9 experimental trials. All SLM factors were found to have a significant effect as their percentage contribution was found to be greater than 5%.
- Laser power showed the highest contribution equal to 83.37%, followed by scan speed and hatch distance equal to 9.92% and 6.7%, respectively.
- The optimal conditions (laser power: 270 W, scan speed: 1000 mm/s and hatch distance: 0.08 mm) determined to yield a lower surface *viz.* Pareto analysis of variance. The determined optimal conditions through statistical analysis are one among the L_9 experiments to yield lower surface roughness with a value equal to $4.11 \mu\text{m}$. Therefore, Taguchi is an effective method to perform analysis and optimize the process.
- The combination of medium and higher scan speed with minimum hatch distance resulted in lower surface roughness. Excess values of laser power might result in remelting of already solidified surface and evaporation, the burnt layer on the top surface creates large irregularities and pores resulting in higher surface roughness. Higher scan speed may not cause evaporation and remain liquid for a small duration with better viscosity to fill the pores present (if any) on the metal surface resulting in lower surface roughness on the build parts. At low values of hatch distance, the overlap between the melt track remains stable and ensures a smooth surface on the build parts.

6.0 References

1. Gao W, Zhang Y, Ramanujan D, Ramani K, Chen Y, Williams CB, Wang CCL, Shin YC, Zhang S, Zavattieri PD. The status, challenges, and future of additive manufacturing in engineering. *Computer-Aided Design*. 2015; 69:65-89. <https://doi.org/10.1016/j.cad.2015.04.001>
2. Wong KV, Hernandez A. A review of additive manufacturing. *International scholarly research notices*. 2012. <https://doi.org/10.5402/2012/208760>
3. Wang JC, Dommati H, Hsieh SJ. Review of additive manufacturing methods for high-performance ceramic materials. *The International Journal of Advanced*

- Manufacturing Technology. 2019; 103(5):2627-47. <https://doi.org/10.1007/s00170-019-03669-3>
4. Thiyaneshwaran N, Pon Selvan C, Lakshmikanthan A, Sivaprasad K, Ravisankar B. Comparison based on specific strength and density of in-situ Ti/Al and Ti/Ni metal intermetallic laminates. *Journal of Materials Research and Technology-Elsevier*. 2021; 14: 1126-36. <https://doi.org/10.1016/j.jmrt.2021.06.102>
 5. Haase C, Bültmann J, Hof J, Ziegler S, Bremen S, Hinke C, Schwedt A, Prah U, Bleck W. Exploiting process-related advantages of selective laser melting to produce high-manganese steel. *Materials*. 2017; 10(1):56. <https://doi.org/10.3390/ma10010056> PMID:28772416 PMCID: PMC5344585
 6. Ardila LC, Garcíandia F, González-Díaz JB, Álvarez P, Echeverría A, Petite MM, Deffley R, Ochoa J. Effect of IN718 recycled powder reuse on properties of parts manufactured using selective laser melting. *Physics Procedia*. 2014; 56:99-107. <https://doi.org/10.1016/j.phpro.2014.08.152>
 7. Vaithilingam J, Goodridge RD, Hague RJ, Christie SD, Edmondson S. The effect of laser remelting on the surface chemistry of Ti6Al4V components fabricated by selective laser melting. *Journal of Materials Processing Technology*. 2016; 232:1-8. <https://doi.org/10.1016/j.jmatprotec.2016.01.022>
 8. Boschetto A, Bottini L, Pilone D. Effect of laser remelting on surface roughness and microstructure of AlSi10Mg selective laser melting manufactured parts. *The International Journal of Advanced Manufacturing Technology*. 2021; 113(9):2739-59. <https://doi.org/10.1007/s00170-021-06775-3>
 9. Prashanth KG. Selective laser melting: materials and applications. *Journal of Manufacturing and Materials Processing*. 2020; 4(1):13. <https://doi.org/10.3390/jmmp4010013>
 10. Murayama M, Hono K, Katayama Y. Microstructural evolution in a 17-4 PH stainless steel after ageing at 400 C. *Metallurgical and Materials Transactions A*. 1999; 30(2):345-53. <https://doi.org/10.1007/s11661-999-0323-2>
 11. Bressan JD, Daros DP, Sokolowski A, Mesquita RA, Barbosa CA. Influence of hardness on the wear resistance of 17-4 PH stainless steel evaluated by the pin-on-disc testing. *Journal of Materials Processing Technology*. 2008; 205(1-3):353-9. <https://doi.org/10.1016/j.jmatprotec.2007.11.251>
 12. Uddin MJ, Siller HR, Mirshams RA, Byers TA, Rout B. Effects of proton irradiation on nanoindentation strain-rate sensitivity and microstructural properties in L-PBF 17-4 PH stainless steels. *Materials Science and Engineering: A*. 2022; 837:142719. <https://doi.org/10.1016/j.msea.2022.142719>
 13. Sabooni S, Chabok A, Feng SC, Blaauw H, Pijper TC, Yang HJ, Pei YT. Laser powder bed fusion of 17-4 PH stainless steel: A comparative study on the effect of heat treatment on microstructure evolution and mechanical properties. *Additive Manufacturing*. 2021; 46:102176. <https://doi.org/10.1016/j.addma.2021.102176>
 14. Sheshadri R, Nagaraj M, Lakshmikanthan A, Patel M, Chandrashekarappa G, Pimenov DY, Giasin K, Prasad R, Wojciechowski S. Experimental investigation of selective laser melting parameters for higher surface quality and microhardness properties: Taguchi and super ranking concept approaches. *Journal of Materials Research and Technology-Elsevier*. 2021; 14:2586-600. <https://doi.org/10.1016/j.jmrt.2021.07.144>
 15. Strano G, Hao L, Everson RM, Evans KE. Surface roughness analysis, modelling and prediction in selective laser melting. *Journal of Materials Processing Technology*. 2013; 213(4):589-97. <https://doi.org/10.1016/j.jmatprotec.2012.11.011>
 16. Charles A, Elkaseer A, Thijs L, Hagenmeyer V, Scholz S. Effect of process parameters on the generated surface roughness of down-facing surfaces in selective laser melting. *Applied Sciences*. 2019; 9(6):1256. <https://doi.org/10.3390/app9061256>
 17. Maamoun AH, Xue YF, Elbestawi MA, Veldhuis SC. Effect of selective laser melting process parameters on the quality of all alloy parts: Powder characterization, density, surface roughness, and dimensional accuracy. *Materials*. 2018; 11(12):2343. <https://doi.org/10.3390/ma11122343> PMID:30469468 PMCID: PMC6316851
 18. Tian Y, Tomus D, Rometsch P, Wu X. Influences of processing parameters on surface roughness of Hastelloy X produced by selective laser melting. *Additive Manufacturing*. 2017; 13:103-12. <https://doi.org/10.1016/j.addma.2016.10.010>
 19. Yang T, Liu T, Liao W, MacDonald E, Wei H, Chen X, Jiang L. The influence of process parameters on vertical surface roughness of the AlSi10Mg parts fabricated by selective laser melting. *Journal of Materials Processing Technology*. 2019; 266:26-36. <https://doi.org/10.1016/j.jmatprotec.2018.10.015>

20. Chate GR, Patel GCM, Parappagoudar MB, Deshpande AS. Application of statistical modelling and evolutionary optimization tools in resin-bonded moulding sand system. In Handbook of research on investigations in artificial life research and development. IGI Global. 2018; 123-52. <https://doi.org/10.4018/978-1-5225-5396-0.ch007>
21. Chate GR, Patel GCM, Harsha HM, Urankar SU, Sanadi SA, Jadhav AP, Hiremath S, Deshpande AS. Sustainable machining: Modelling and optimization using Taguchi, MOORA and DEAR methods. Materials Today: Proceedings. 2021; 46:8941-7. <https://doi.org/10.1016/j.matpr.2021.05.365>
22. Patel GCM, Shettigar AK, Parappagoudar MB. A systematic approach to model and optimize the wear behaviour of castings produced by the squeeze casting process. Journal of Manufacturing Processes. 2018; 32:199-212. <https://doi.org/10.1016/j.jmapro.2018.02.004>
23. Patel GCM, Shettigar AK, Krishna P, Parappagoudar MB. Backpropagation genetic and recurrent neural network applications in modelling and analysis of squeeze casting process. Applied Soft Computing. 2017; 59:418-37. <https://doi.org/10.1016/j.asoc.2017.06.018>
24. Leon A, Aghion E. Effect of surface roughness on corrosion fatigue performance of AlSi10Mg alloy produced by Selective Laser Melting (SLM). Materials Characterization. 2017; 131:188-94. <https://doi.org/10.1016/j.matchar.2017.06.029>
25. Wang Z, Xiao Z, Tse Y, Huang C, Zhang, W. Optimization of processing parameters and establishment of a relationship between microstructure and mechanical properties of SLM titanium alloy. Optics and Laser Technology. 2019; 112:159-67. <https://doi.org/10.1016/j.optlastec.2018.11.014>
26. Sun Y, Bailey R, Moroz A. Surface finish and properties enhancement of selective laser melted 316L stainless steel by surface mechanical attrition treatment. Surface and Coatings Technology. 2019; 378:124993. <https://doi.org/10.1016/j.surfcoat.2019.124993>
27. Jamshidi P, Aristizabal M, Kong W, Villapun V, Cox SC, Grover LM, Attallah MM. Selective laser melting of Ti-6Al-4V: The impact of post-processing on the tensile, fatigue and biological properties for medical implant applications. Materials. 13(12):2813. <https://doi.org/10.3390/ma13122813> PMID:32580477 PMCID: PMC7345457
28. Nowacki J. Weldability of 17-4 PH stainless steel in centrifugal compressor impeller applications. Journal of Materials Processing Technology. 2004; 157:578-83. <https://doi.org/10.1016/j.jmatprotec.2004.07.117>
29. Mutlu I, Oktay E. Influence of the fluoride content of artificial saliva on metal release from 17-4 PH stainless steel foam for dental implant applications. Journal of Materials Science and Technology. 2013; 29(6):582-8. <https://doi.org/10.1016/j.jmst.2013.03.006>
30. Nie S, Lou F, Ji H, Yin F. Tribological performance of CF-PEEK sliding against 17-4PH stainless steel with various cermet coatings for water hydraulic piston pump application. Coatings. 2019; 9(7):436. <https://doi.org/10.3390/coatings9070436>
31. Mirzadeh H, Najafizadeh A, Moazeny M. Flow curve analysis of 17-4 PH stainless steel under hot compression test. Metallurgical and Materials Transactions A. 2009; 40(12):2950-8. <https://doi.org/10.1007/s11661-009-0029-5>
32. Shishkovsky I, Morozov Y, Smurov I. Nanostructural self-organization under selective laser sintering of exothermic powder mixtures. Applied Surface Science. 2009; 255(10):5565-8. <https://doi.org/10.1016/j.apsusc.2008.09.090>
33. Matras A. Research and optimization of surface roughness in milling of SLM semi-finished parts manufactured by using different laser scanning speeds. Materials. 2019; 13(1):9. <https://doi.org/10.3390/ma13010009> PMID:31861370 PMCID: PMC6981844
34. Kabir MR, Richter H. Modeling of processing-induced pore morphology in an additively manufactured Ti-6Al-4V alloy. Materials. 2017; 10(2):145. <https://doi.org/10.3390/ma10020145> PMID:28772504 PMCID: PMC5459110
35. Safdar A, He HZ, Wei LY, Snis A, de Paz LEC. Effect of process parameters settings and thickness on surface roughness of EBM produced Ti-6Al-4V. Rapid Prototyping Journal. 2012. <https://doi.org/10.1108/13552541211250391>
36. Foster SJ, Carver K, Dinwiddie RB, List F, Unocic KA, Chaudhary A, Babu SS. Process-defect-structure-property correlations during laser powder bed fusion of alloy 718: Role of *in situ* and *ex-situ* characterizations. Metallurgical and Materials Transactions A. 2018; 49(11):5775-98. <https://doi.org/10.1007/s11661-018-4870-2>

Nomenclature

SLM: Selective Laser Melting

SFL: Sum at Factor Levels

SSD: Sum of Squares of Differences

PC: Per cent Contribution

AM: Additive Manufacturing

S/N ratio: Signal to Noise ratio

LP: Laser Power

SS: Scan Speed

H_d : Hatch Distance

R_a : Surface Roughness